TRANSITION IN MHD CHANNEL FLOW WITH SPANWISE MAGNETIC FIELD

Thomas Boeck, Dmitry Krasnov
Fakultät Maschinenbau,
Technische Universität Ilmenau
Postfach 100565, 98684 Ilmenau, Germany
thomas.boeck@tu-ilmenau.de, dmitry.krasnov@tu-ilmenau.de

Maurice Rossi
Institut Jean Le Rond D'Alembert,
Université Pierre et Marie Curie,
4 place Jussieu, F-75252 Paris Cedex 05, France
maur@ccr.jussieu.fr

Oleg Zikanov
Department of Mechanical Engineering,
University of Michigan - Dearborn,
4901 Evergreen Road, Dearborn, MI 48128-1491, USA
zikanov@umich.edu

ABSTRACT

The linear and nonlinear evolution of perturbations is studied in a magnetohydrodynamic channel flow with electrically insulating channel walls in which a strong magnetic field possesses an orientation orthogonal to the stream but parallel to the walls. The basic flow is unaffected by the magnetic field and retains the Poiseuille velocity profile. Linear optimal perturbation and their maximum amplifications over finite time intervals are computed using an iterative scheme based on the direct and adjoint governing equations for the subcritical Reynolds number $Re = 5000$. The presence of a magnetic field changes the spatial structure of optimal perturbations. As the Hartmann number increases, the optimal modes cease to be the classical streamwise rolls and become oblique rolls with axes at some angle to the direction of the flow. At sufficiently high Hartmann numbers, the optimal perturbations are the purely spanwise Orr modes. For Hartmann numbers in the range from 0 to 100 direct numerical simulations (DNS) are applied to investigate how the transition to turbulence is affected by the magnetic field. Simulations are conducted using the optimal modes as initial values with weak three-dimensional noise added at the maximum amplification time.

INTRODUCTION

A channel flow in a purely spanwise magnetic field represents important aspects of complex flows in the presence of a magnetic field with non-zero component parallel to solid walls. Such flows can be found in numerous metallurgical and materials processing applications. Prominent examples include the electromagnetic flow control in continuous steel casting (Davidson, 1999; Thomas & Zhang, 2001) and in growth of large silicon crystals. Another area of applications is the liquid metal (Li or Pb-17Li) cooling blankets of breeder type for fusion reactors (Barleon *et al.*, 2001). The typical blanket design includes a duct flow in a strong imposed magnetic field. Instability and transition to turbulence in sidewall boundary layers (in respect to which the magnetic field is spanwise) is one of the possible ways to achieve the desired intensification of heat and mass transfer. From a different application viewpoint, Lee & Choi (2001) have shown that a spanwise magnetic field can lead to substantial reduction of the turbulent drag in a channel flow.

The general effect of the imposed magnetic field is twofold. On the one hand, the flow is suppressed by Joule dissipation of induced electric currents. On the other hand, the magnetic field acts anisotropically. The Lorentz force preferentially affects the flow modes with strong gradients in the direction of the magnetic field. No electric currents are generated and no Joule dissipation occurs in a two-dimensional flow uniform along the magnetic field lines.

As far as general theory of instability and transition to turbulence in parallel shear flows is concerned, the situation of a channel in a spanwise field is of substantial interest. The applied magnetic field renders the spanwise direction preferable in the sense that the perturbations uniform in this direction are not directly affected, in particular, not suppressed by the magnetic field. We examine this aspect in detail through a systematic study of the optimal linear perturbations providing the strongest transient growth for different strength of the magnetic field for a fixed, subcritical Reynolds number. Among the possible transition scenarios, we focus on the one based on the algebraic transient growth of optimal perturbations and their subsequent three-dimensional breakdown, which we shall study by direct numerical simulations. This scenario was shown to realize in other parallel shear flows, such as the plane Poiseuille (Reddy *et al.*, 1998), pipe Poiseuille (Zikanov, 1996), and Hartmann (Krasnov *et al.*, 2004) flows. We shall discuss the results of our study after presenting the mathematical model and the numerical methods in the next section.

PROBLEM DEFINITION AND NUMERICAL APPROACH

We consider the flow of an incompressible electrically conducting fluid in an infinite plane channel between insulating walls located at $z = \pm L$ with a magnetic field $\boldsymbol{B}_0 = B_0\boldsymbol{e}$ in the spanwise direction $\boldsymbol{e} \equiv (0, 1, 0)$. The principal sketch of the problem is shown in figure 1.

The flow is driven by a pressure gradient $\partial P_0/\partial x$. We apply the quasi-static approximation, whereby the fluctuations

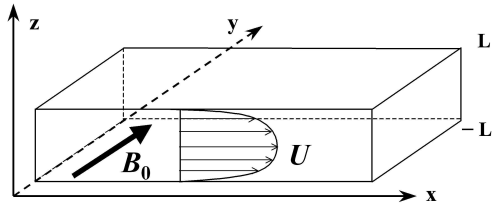

Figure 1: Channel flow under uniform spanwise magnetic field.

of the magnetic field arising due to the fluid motion adjust instantaneously to the velocity fluctuations and are much weaker than the imposed magnetic field. This approach corresponds to the limit of low magnetic Reynolds number Re_m and approximates the case of liquid metal flows. This approximation is widely used to study turbulent MHD channel flows, e.g. by Lee & Choi (2001); Boeck *et al.* (2007). The length and velocity scales are the laminar centerline velocity U and the channel half width L. The unit of time is L/U. The non-dimensional basic velocity profile is the parabolic Poiseuille profile $U_H = 1 - z^2$. We introduce two non-dimensional parameters, the Reynolds number

$$Re = UL/\nu \tag{1}$$

and the Hartmann number

$$Ha = B_0 L\sqrt{\sigma/\rho\nu}, \tag{2}$$

where ρ and ν stand for density and kinematic viscosity of the fluid, and σ denotes its electric conductivity.

Thereby, the governing equations in non-dimensional form reduce to the Navier-Stokes system with the additional Lorentz force, i.e.

$$\frac{\partial \boldsymbol{v}}{\partial t} + (\boldsymbol{v}\cdot\nabla)\boldsymbol{v} = -\nabla p + \frac{1}{Re}\nabla^2\boldsymbol{v} + \tag{3}$$
$$+N\left(-\nabla\phi\times\boldsymbol{e} + (\boldsymbol{v}\times\boldsymbol{e})\times\boldsymbol{e}\right),$$
$$\nabla\cdot\boldsymbol{v} = 0, \tag{4}$$
$$\nabla^2\phi = \nabla\cdot(\boldsymbol{v}\times\boldsymbol{e}), \tag{5}$$
$$v_x = v_y = v_z = \frac{\partial\phi}{\partial z} = 0 \quad \text{at } z = \pm 1 \tag{6}$$

with the magnetic interaction parameter $N \equiv Ha^2/Re$ and the electric potential denoted as ϕ.

Finally, integral conditions should be specified. We assume that the volume flux Q per span width is constant. In addition, the total electric current is set to zero in the y-direction, which fixes the mean potential gradient in the y-direction.

Linear analysis of non-modal perturbations

In the linear analysis we split the flow fields into a basic flow and three-dimensional perturbations as

$$\boldsymbol{v} = U_H(z)(1,0,0) + \boldsymbol{v}_p, \quad \phi = \phi_H + \phi_p(x,y,z), \tag{7}$$
$$p = P_H + p_p.$$

We linearize the system (3–5) with respect to the perturbations and study the evolution of decoupled monochromatic Fourier modes with the wavenumbers α and β in the streamwise (x) and spanwise (y) directions at $Re = 5000$ and various values of Ha. For this given Reynolds number the flow is linearly stable, i.e. all eigensolutions decay exponentially. However, the eigenmodes may form combinations that experience substantial transient algebraic growth before they eventually decay.

To quantify the amplification at time T we use the kinetic energy E of the perturbations, whereby the individual contributions of each wavenumber pair (α,β) can be considered independently. This norm, therefore, is defined as

$$E(T) \equiv \int (\hat{u}(z,T)\hat{u}^+(z,T) + \hat{v}(z,T)\hat{v}^+(z,T) + \tag{8}$$
$$+\hat{w}(z,T)\hat{w}^+(z,T))\mathrm{d}z$$

where the superscript + denotes complex conjugation. Spatial integration is performed over the entire channel width, and the perturbations are obtained by time integration over the time period $[0,T]$.

The amplification gain of any given mode at time T is the ratio $E(T)/E(0)$. This ratio can be maximized over all possible initial vertical shapes to give the maximum amplification $\hat{G}(T,\alpha,\beta)$ of the disturbances with the wavenumbers (α,β) at the time T. The search for the disturbance providing the maximum amplification, the so-called optimal disturbance, is the subject of this part of our study. To solve this problem we apply a method which computes the maximum energy gain through an optimization procedure (e.g., Farrell & Ioannou (1996); Andersson *et al.* (1999); Luchini (2000); Schmid & Henningson (2001)). The optimum of $E(T)/E(0)$ is determined with two imposed constraints: (i) the disturbance energy $E(0)$ at time $t = 0$ is equal to unity; (ii) the disturbance satisfies the linear governing equations as well as the boundary conditions during the complete time interval $[0,T]$. The solution is obtained with the help of a Lagrangian formalism in which Lagrangian multipliers – adjoint fields – are introduced to enforce these constraints. The entire procedure, therefore, amounts to a series of forth-and-back iterations solving direct ($0 \to T$) and adjoint ($T \to 0$) equations.

The direct and adjoint equations are solved numerically using a pseudospectral method based on Chebyshev polynomials and a projection approach to enforce incompressibility. The code is based on the one used by Schmid & Rossi (2004) and has been adapted to the MHD channel flow.

Method of direct numerical simulations

We study instability and transition to turbulence triggered by the non-linear evolution of optimal perturbations, obtained and analysed previously in the linear context. To reproduce the non-linear flow evolution, direct numerical simulations are employed. The non-dimensional equations (3–5) with boundary conditions (6) are solved numerically. We use a representation of the flow field in terms of velocity potentials complying with the incompressibility constraint and a pseudo-spectral algorithm. The pseudospectral method is based on Fourier series in the horizontal directions x and y and a Chebyshev polynomial expansion in the vertical z–direction (Canuto *et al.*, 1988; Gottlieb & Orszag, 1977). This representation, therefore, accounts for periodic boundary conditions in the horizontal direction and no-slip conditions in the wall-normal direction.

We have applied this method and the corresponding flow solver in our previous studies, e.g., Krasnov *et al.* (2004); Boeck *et al.* (2007). The modifications made for the present work concern the Lorentz force and the time-stepping method. The Lorentz force term is modified to spanwise orientation of the magnetic field and is treated as an explicit term in the temporal discretization. Furthermore, the new time-stepping scheme uses three time levels for the approximation of the time derivative and is second-order accurate. The flow solver is parallelized. Inter-process communication utilizes the MPI library. More details can be found in Boeck *et al.* (2007).

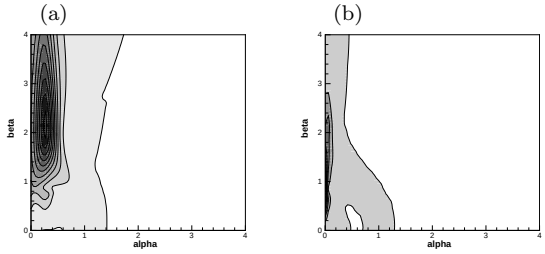

Figure 2: Isolevels of energy amplification $\hat{G}(\alpha, \beta, T)$ in the (α,β)-plane for $Re = 5000$ and $Ha = 10$. Two typical times T: (a) $T = T_{opt} \approx 64$, at which the global maximum is reached, (b) $T \approx 189$, corresponding to the optimal time for purely streamwise perturbations (also see figure 3).

RESULTS

Linear evolution results

In this section, we investigate how the transient growth changes in the presence of a spanwise magnetic field. The optimization method computes the maximum energy amplification $\hat{G}(\alpha, \beta, T, Re, Ha)$ for a given wavenumber pair (α, β) and a given time T. This function itself can be maximized over α and β to provide $\hat{M}_{tot}(T, Re, Ha)$ – the maximum amplification among all the perturbations at given time T and flow parameters. Further maximization over time T provides the global maximum amplification $M_{tot}(Re, Ha)$ which is reached at time $T = T_{opt}(Re, Ha)$. The corresponding optimal wavenumber pair is denoted by $(\alpha_{opt}, \beta_{opt})$.

For the purely streamwise perturbations, when the function $\hat{G}(\alpha, \beta, T, Re, Ha)$ is maximized over β, provided that $\alpha = 0$, equivalent optimal quantities may also be defined: $M_{stream}(Re, Ha)$ and β_{stream}.

The search for optimal perturbations is performed in a square (α, β)-domain (a β-interval in the case of streamwise perturbations) with the wavenumbers varying from 0 to 4.

Typical behaviour of the amplification factor $\hat{G}$ is illustrated in figures 2. Isolines of $\hat{G}(\alpha, \beta, T, Re, Ha)$ are shown as functions of α and β at different times T for $Re = 5000$ and Hartmann number $Ha = 10$. The contours indicate variation of $\hat{G}$ from low (white regions) to high (black regions) values.

The largest transient amplification for hydrodynamic channel flow is provided by perturbations with $\alpha = 0$, as shown, e.g., by Butler & Farrell (1992). In that case, the optimal perturbations have the form of purely streamwise vortices. When the spanwise magnetic field is applied, these modes are strongly damped, and are therefore taken over by oblique modes with non-zero wavenumber α. In particular, we found that at Hartmann numbers between 2 and 5 the strongest transient growth is already provided by oblique perturbations with $\alpha \neq 0$. This constitutes the main difference between the magnetic and non-magnetic cases.

For $Ha = 10$, which represents the cases of small and moderate Hartmann numbers, there is a single peak of the amplification curve corresponding to an oblique mode at $T_{opt} \approx 64$ (see figure 3). For large times T ($T > 189$), the streamwise perturbations dominate. It has to be stressed that the effect of the magnetic field is quite strong even at such a small Hartmann number. The global maximum $M_{tot}(Re, Ha)$ observed for an oblique mode at T_{opt} is about twice as large as the maximum amplification $M_{stream}(Re, Ha)$ obtained at $T \approx 189$ for the streamwise modes: $M_{tot} \approx 900$ vs. $M_{stream} \approx 450$.

The effect of higher Hartmann number may render the picture more complex, as can be seen in figure 4 for $Ha = 50$. The highest amplification occurs for $T \approx 15$ (fig. 4a), but at later stages, e.g. at $T \approx 28$, several co-existing local maxima are observed (fig. 4b). The entire effect is illustrated further in fig. 4c. Again, streamwise modes dominate at large T, but the curve of maximum amplification shows three discernable peaks corresponding to the global maximum at $T_{opt} \approx 15$ and two local maxima at $T \approx 33$ and $T \approx 88$. These peaks are associated with the dominance of different families of oblique modes with different (α,β) wavenumbers.

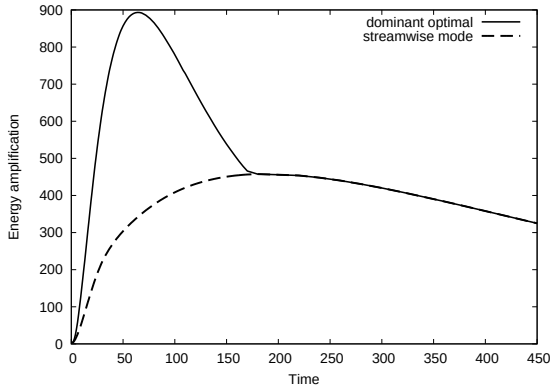

Figure 3: Energy amplification factors $\hat{M}_{tot}(T, Re, Ha)$ (———) for dominant modes and $\hat{M}_{stream}(T, Re, Ha)$ for streamwise vortices (- - - -) as functions of time T; $Re = 5000$ and $Ha = 10$.

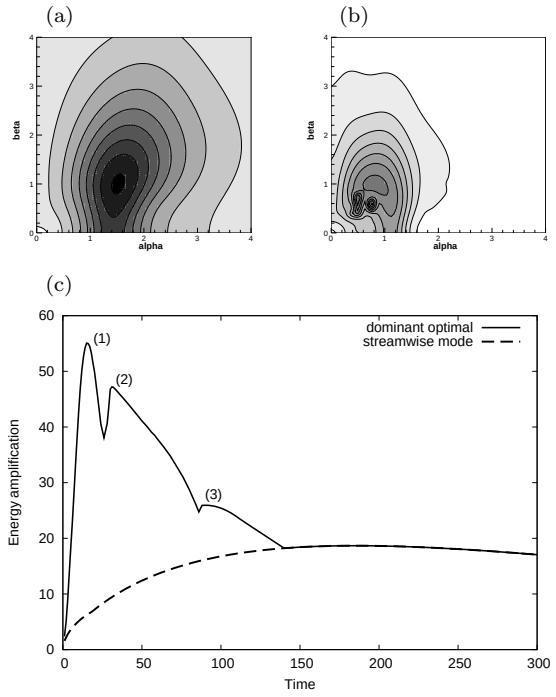

Figure 4: The results of linear analysis for $Re = 5000$ and $Ha = 50$. (a,b) Isolevels of energy amplification $\hat{G}(\alpha, \beta, T)$ in the (α,β)-plane at different moments in time T – (a) global maximum at $T = 15$, (b) three local peaks at $T \approx 28$. (c) Amplification factors $\hat{M}_{tot}(T, Re, Ha)$ (———) for dominant modes and $\hat{M}_{stream}(T, Re, Ha)$ for streamwise vortices (- - - -) as functions of time T.

The effect of the magnetic field on the transient growth is summarized in figures 5 and 6. Maximization with respect to T and the two wavenumbers α and β provides the maximum amplification $\hat{M}$ and the corresponding wavevector (α, β) as functions of Ha. We see that the transient growth of oblique perturbations is also reduced by the spanwise magnetic field,

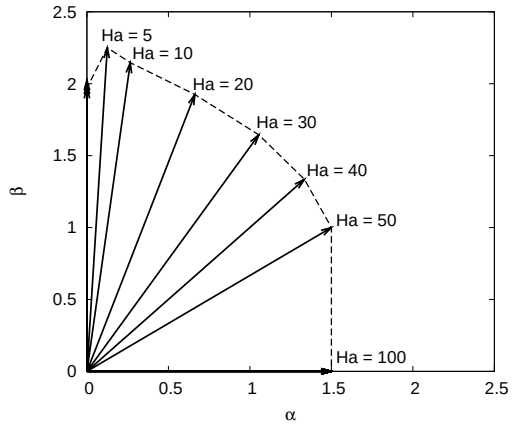

Figure 5: Optimal wavevector $(\alpha_{opt}, \beta_{opt})$ vs. Hartmann number Ha for $Re = 5000$.

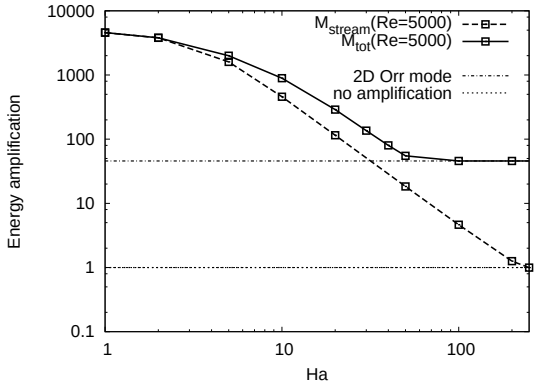

Figure 6: Maximum amplification factors M_{tot} and M_{stream} vs. Hartmann number Ha for $Re = 5000$.

and that the oblique angle of the optimal modes increases monotonically with the magnetic field strength.

For $Ha \geq 100$, the spanwise Orr-mode vortices unaffected by the magnetic field become the modes with strongest transient amplification. In Fig. 6, these modes provide the constant amplification level, which is maintained for $Ha \geq 100$. We also show the maximum amplification of purely streamwise rolls with $\alpha = 0$ for comparison. For these modes, the amplification $\hat{M}_{stream}$ eventually reduces to unity, i.e. they experience no transient growth for sufficently large Ha.

Summarizing the results obtained at $Re = 5000$, we can conclude that the largest amplification is found (i) for streamwise modes at very small Hartmann number $Ha < 5$, (ii) for oblique modes in a wide range of moderate to large Ha, and (iii) for purely spanwise modes at very large Ha, greater than 100.

Concerning the damping of streamwise perturbations, we note that scaling relations $\hat{M}_{stream} \sim Ha^{-2}$ (cf. figure 6) and $\beta \sim Ha^{-1}$ are found numerically. The scaling of $\hat{M}_{stream}$ can be derived by an asymptotic analysis of the linearized Navier-Stokes equations. Details are given in Krasnov *et al.* (2007).

Non-linear evolution and transition to turbulence

In this section we study the non-linear evolution for flow regimes with subcritical $Re = 5000$ and Ha ranging between 10 and 100 by DNS. The transition to turbulence is considered for the classical two-step scenario. This scenario implies that the initial transient growth of optimal perturbations is sufficiently strong to render the modulated basic flow unstable to three-dimensional perturbations.

The initial conditions for the DNS consist of the basic flow modulated by an optimal linear mode of a specified amplitude. For each Hartmann number we choose the corresponding optimal mode found in the linear problem. If different linear modes give maximum amplifications at different times, such as in the $Ha = 50$ case, simulations are conducted separately for every mode used as an initial condition. Besides that, we also examine purely streamwise vortices to reveal their diminishing role in transition as Ha increases. The initial kinetic energy of the optimal perturbations $E(0)$ is specified between 10^{-5} and 10^{-2} relative to the energy of the basic flow. To trigger the transition, weak three-dimensional noise is added to the modulated flow at the time $t = T_{opt}$ of maximum linear amplification. The energy E_{3D} of the noise is chosen to be 10^{-2} of the initial optimal perturbation energy.

Transition by streamwise and oblique modes

We recall that for the non-magnetic case the linear analysis yields streamwise vortices as optimal perturbations. Indeed, our simulations at $Ha = 0$ show that a small initial energy $E(0) = 10^{-5}$ is sufficient for the flow to become turbulent when 3D noise is added. For higher Ha this is not the case anymore – there is a significant effect of the magnetic field upon the streamwise vortices already at $Ha = 10$. As can be seen in figure 7(top), transition to turbulence is induced when a perturbation energy of streamwise modes exceeds the level of 10^{-3}. At the same time, the results of the optimal oblique mode in figure 7(bottom) show that it is a far better candidate to trigger the transition. Even an initial energy as small as $E(0) = 10^{-5}$ is already sufficient when 3D noise is added. Moreover, the transition itself occurs earlier than in the case of streamwise vortices.

The two-step mechanism of transition was applied for the set of Hartmann numbers in figure 5 up to $Ha = 100$. We have considered all families of optimal linear modes, each providing the maximum amplification in a certain time range (e.g., figure 4). No transition to turbulence was detected starting at $Ha = 30$ and higher values of Ha. The nonlinear effects become noticeable when the initial perturbation energy becomes $E(0) \geq 10^{-3}$, but the transition to turbulence is never triggered. The possible explanation is two-fold. First, the maximum energy amplification gets weaker as Ha grows (for example, only $M_{tot} \approx 55$ for $Ha = 50$). Secondly, the Joule dissipation strongly suppresses the three-dimensional perturbations once they are introduced.

Transition caused by Orr modes

At high Hartmann numbers ($Ha \geq 100$, figures 5 and 6), the transient amplification is provided by the Orr modes unaffected by the magnetic field. Their nonlinear growth at Reynolds number $Re = 5000$ can sufficiently modify the basic flow to make it unstable to 3D noise. Therefore, the Orr modes can still be considered as a possible route to turbulence. At the same time, the results observed in the previous section suggest that 3D evolution would be suppressed by a strong magnetic field.

We conducted simulations at $Ha = 100$ with the 2D Orr mode being the optimal perturbation. It was found that sufficiently strong initial perturbations $E(0) \geq 10^{-3}$ (figure 8a) evolve into a purely two-dimensional travelling-wave state observed earlier by Jimenez (1990) in a two-dimensional non-magnetic channel flow. This evolution can be regarded as a common solution for all values of Ha, including the non-magnetic case. In the latter case, the transition to a fully turbulent state is triggered by 3D noise added at

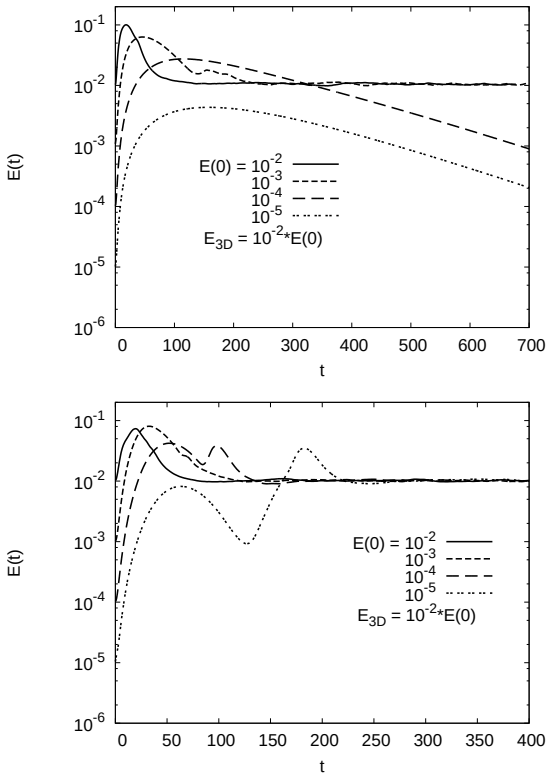

Figure 7: The nonlinear evolution of perturbation energy $E(t)$ at $Re = 5000$ and $Ha = 10$ starting with streamwise optimal mode (top) and starting with an optimal oblique mode (bottom). Initial energy of optimal modes varies from $E(0) = 10^{-5}$ to $E(0) = 10^{-2}$, the $3D$ noise of energy $E_{3D} = 10^{-2}E(0)$ is added at $t = T_{opt}$.

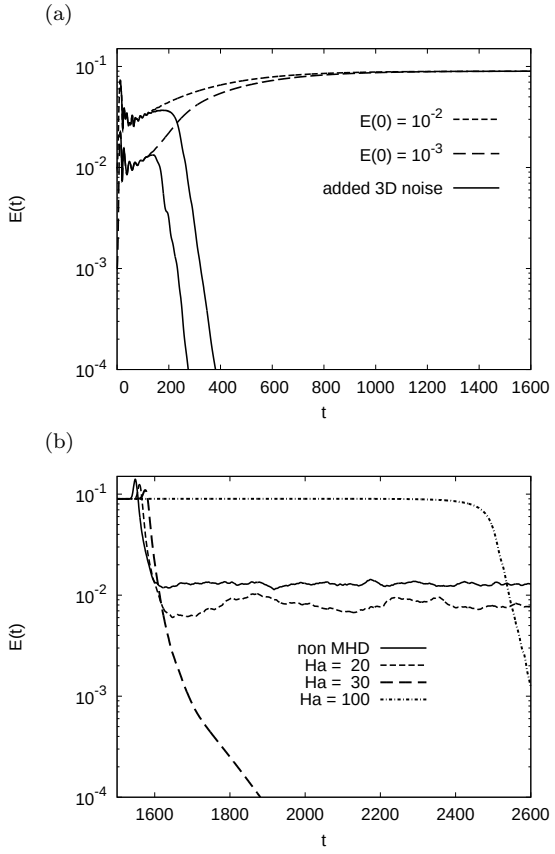

Figure 8: The nonlinear evolution of perturbation energy $E(t)$ starting with the Orr mode at $Re = 5000$ and different Ha. (a) Case $Ha = 100$, the evolution with intial energies $E(0) = 10^{-3}$ and 10^{-2} up to a sustained $2D$ finite-amplitude state. $3D$ noise of energy $E_{3D} = 10^{-2}E(0)$ is added at $t = T_{opt}$ for the bold curves. (b) Instability of the sustained $2D$ state and transient evolutions for $0 \leq Ha \leq 100$, $3D$ noise of amplitude $E_{3D} = 10^{-7}E_{2Dstate}$ being added at $T \approx 1500$. Curves at $Ha = 0,\ 20,\ 30,\ 100$ are presented.

$t = T_{opt}$. Contrary to that, at $Ha = 100$ the noise destroys the time-dependent 2D flow in such a way that it returns back to the basic unperturbed state, as seen in figure 8a (solid curves). This re-laminarization can be attributed to energy transfer by nonlinear interactions from the 2D modes to 3D modes with a finite spanwise wavenumber, which are rapidly damped by the Joule dissipation.

Similar simulations were conducted in the entire range $0 \leq Ha \leq 100$. A re-laminarization similar to that for $Ha = 100$ was found at $Ha \geq 30$. Transition to turbulence was found at lower Ha (e.g. at $Ha = 10$ and 20). We note, that at such Hartmann numbers, transition was also produced by the oblique modes. One can conclude that, in the presence of a sufficiently strong magnetic field, the Orr modes cannot be considered as the route to 3D turbulence.

Another aspect of the results obtained at $Ha = 100$ is the question of whether purely two-dimensional turbulence can be sustained by a strong imposed magnetic field (see, e.g., a discussion in Tsinober (1990)). Such 2D states are known to be very unstable in respect to random perturbations, so that non-MHD flow becomes 3D turbulent very rapidly as the perturbations are introduced. In the presence of the magnetic field the situation may change. This raises some questions such as (i) whether the 2D states are stable to 3D perturbations and, (ii) if unstable, towards which flow regime they evolve.

We continued two simulations with $E(0) = 10^{-3}$ and 10^{-2} as two-dimensional until the finite-amplitude 2D solutions similar to those found by Jimenez (1990) were obtained (see figure 8). Adding 3D noise at this stage ($T \approx 1500$) led to the instability of the 2D structures and quick energy drain into 3D perturbations. In case of $Ha \leq 20$ a transition to turbulence was detected (figure 8b, non MHD and $Ha = 20$ curves). For higher Hartmann number, as $Ha \geq 30$, any development of 3D structures was suppressed by the strong magnetic field. As a result, the flow evolved back to the basic state (curves for $Ha = 30$ and 100 in figure 8b). Concluding this section, we can state that whereas a sufficiently strong magnetic field eventually suppresses any three-dimensionality in the flow, it cannot sustain the non-steady 2D solutions found by Jimenez (1990).

CONCLUSIONS

We have studied instability and transition to turbulence in a plane channel flow of an electrically conducting fluid in the presence of a uniform constant magnetic field in the spanwise direction. The case of small magnetic Reynolds number was considered. The scenario of transition based on the transient growth of certain perturbations and subsequent secondary instability of the modified base flow was analyzed using linear and non-linear computational models. In the linear part, the optimal (with strongest transient growth) perturbations were determined with the help of the iterative procedure based on integration of direct and adjoint equations. The non-linear evolution of the optimal modes, their breakdown, and transition to turbulence were investigated in a series of direct numerical simulations.

We found that the magnetic field has strong quantitative and qualitative effects on the transient growth. By means of added Joule dissipation, it suppresses all perturbations except purely spanwise modes. For the streamwise rolls that appear as optimal perturbations in the classical hydrodynamic flow, the suppression is described by power law dependencies with the energy amplification and spanwise wavenumber of the strongest growing mode scaling as Ha^{-2} and Ha^{-1}, respectively.

More interestingly, the nature of the optimal modes changes under the impact of the magnetic field. At Hartmann numbers above a moderate threshold value (between $Ha = 2$ and $Ha = 5$), the optimal perturbations change from streamwise to oblique rolls. Their oblique angle increases monotonically with Ha demonstrating the shifting balance between the two opposing energy fluxes, the Joule dissipation and the energy transfer from the basic flow, both of which decrease with the growing oblique angle. At sufficiently strong magnetic field characterized by Ha larger than a threshold between 50 and 100, the strongest (and quite moderate) growth is supplied by purely spanwise Orr modes unaffected by the magnetic field.

In the non-linear analysis we first focused on the transition to turbulence caused by the breakdown of growing streamwise or oblique modes at Hartmann numbers in the range $5 \leq Ha \leq 50$. Numerical experiments were conducted, in which linear optimal modes of low amplitude were used as initial conditions and weak three-dimensional noise was added to trigger the secondary instability. It was found that stronger optimal growth of the oblique modes renders them better candidates for the dominant mechanism of the transition. For example, at $Ha = 10$ and $Re = 5000$, the initial energy not less than 10^{-3} of the energy of the base flow is required by the streamwise modes to initiate the transition, while energy levels as small as 10^{-5} are sufficient for the oblique modes.

In the case of strong magnetic fields at Ha about 100 and higher, the spanwise perturbations are the only ones experiencing appreciable transient growth. We found that these modes are unable to generate the transition to turbulence at high Ha. Their growth and non-linear saturation lead to establishing a spanwise-independent secondary flow observed earlier in the two-dimensional simulations of Jimenez (1990). Instability of this flow to three-dimensional perturbations cannot be suppressed by the magnetic field in the range of Ha considered in the present paper. The instability leads to the transition back into the base state. Further investigations are needed to resolve interesting related questions, such as that of stability of the two-dimensional solutions at even higher Ha and the role played by the spanwise Orr modes in the transition at supercritical Re.

ACKNOWLEDGMENTS

TB and DK acknowledge support by the Deutsche Forschungsgemeinschaft (Grant Bo1668/2-2). OZ acknowledges support from the US Department of Energy (Grant DE FG02 03 ER46062). The cooperation between the University of Michigan – Dearborn and the Technische Universität Ilmenau is supported by the US National Science Foundation (Grant INT 0338713) and DAAD.

REFERENCES

Andersson, P., Berggren, M. & Henningson, D. S. 1999 Optimal disturbances and bypass transition in boundary layers. *Phys. Fluids* **11**, 134–150.

Barleon, L., Burr, U., Mack, K. J. & Stieglitz, R. 2001 Magnetohydrodynamic heat transfer research related to the design of fusion blankets. *Fusion Techn.* **39(2)**, 127–156.

Boeck, T., Krasnov, D. & Zienicke, E. 2007 Numerical study of turbulent magnetohydrodynamic channel flow. *J. Fluid Mech.* **572**, 179–188.

Butler, K. M. & Farrell, B. F. 1992 Three-dimensional optimal perturbations in viscous shear flow. *Phys. Fluids* **4** (8), 1637–1650.

Canuto, C., Hussaini, M. Y., Quateroni, A. & Zang, T. A. 1988 *Spectral Methods in Fluid Dynamics*. Springer Verlag.

Davidson, P. A. 1999 Magnetohydrodynamics in materials processing. *Annu. Rev. Fluid Mech.* **31**, 273–300.

Farrell, B. F. & Ioannou, P. J. 1996 Generalized stability theory part I: autonomous operators. *J. Atmos. Sci.* **53**, 2025–2040.

Gottlieb, D. & Orszag, S. A. 1977 *Numerical Analysis of Spectral Methods*. Philadelphia: SIAM.

Jimenez, J. 1990 Transition to turbulence in two-dimensional Poiseuille flow. *J. Fluid Mech.* **218**, 265–297.

Krasnov, D., Rossi, M., Zikanov, O. & Boeck, T. 2007 Transition to turbulence in channel flow with spanwise magnetic field. *Submitted to J. Fluid Mech.* .

Krasnov, D. S., Zienicke, E., Zikanov, O., Boeck, T. & Thess, A. 2004 Numerical study of instability and transition to turbulence in the Hartmann flow. *J. Fluid Mech.* **504**, 183–211.

Lee, D. & Choi, H. 2001 Magnetohydrodynamic turbulent flow in a channel at low magnetic Reynolds number. *J. Fluid Mech.* **429**, 367–394.

Luchini, P. 2000 Reynolds-number-independent instability of the boundary layer over a flat surface: optimal perturbations. *J. Fluid Mech.* **404**, 289–309.

Reddy, S. C., Schmid, P. J., Bagget, P. & Henningson, D. S. 1998 On the stability of stream-wise streaks and and transition thresholds in plane channel flow. *J. Fluid Mech.* **365**, 269–303.

Schmid, P. J. & Henningson, D. S. 2001 *Stability and Transition in Shear Flows*. Springer Verlag.

Schmid, P. J. & Rossi, M. 2004 Three-dimensional stability of a Burgers vortex. *J. Fluid Mech.* **500**, 103–112.

Thomas, B. G. & Zhang, L. 2001 Mathematical modeling of fluid flow in continuous casting: a review. *ISIJ Intern* **41** (10), 1181–1193.

Tsinober, A. 1990 Mhd flow drag reduction. In *Viscous drag reduction in boundary layers* (ed. D. Bushnell & J. Hefner), pp. 327–349.

Zikanov, O. 1996 On the instability of pipe Poiseuille flow. *Phys. Fluids* **8**, 2923–2932.